JMEPEG (2019) 28:363–371
https://doi.org/10.1007/s11665-018-3769-9

1059-9495/$19.00

Tribo-corrosion and Albumin Attachment of Nitrogen Ion-Implanted CoCrMo Alloy During Friction Onset

Xueyan Yan, Jie Meng, Kewei Gao, Xiaolu Pang, and Alex A. Volinsky

(Submitted May 3, 2018; in revised form November 12, 2018; published online November 26, 2018)

In this paper, CoCrMo alloy surface was implanted with 100 keV nitrogen ions to modify it. Bovine serum albumin (BSA) adsorption and the initial behavior of tribo-corrosion in the simulated system were studied. Nitrogen ion implantation can promote BSA dynamic adsorption due to the change of friction and wear mechanisms. From the tribo-corrosion test results, the open circuit potential (OCP) increased to about 0.6 V and the coefficient of friction (COF) decreased to about 0.2 for the nitrogen ion-implanted CoCrMo compared with the untreated sample before the modified layer failure. The point when the open circuit potential and the coefficient of friction changed during long wear time (1, 2 and 4 h) is considered the sign of the worn through modified layer. Then, the OCP of the implanted sample rose by 0.3 V compared with the untreated sample, and the COF remained at around 0.3, which is lower compared with the COF of untreated sample after the modified layer has been worn through. Thus, nitrogen ion implantation not only improved wear and corrosion resistance of the CoCrMo alloy, but also promoted BSA adsorption on the CoCrMo alloy surface, which effectively reduced the wear volume and metal ions release.

Keywords BSA adsorption, CoCrMo alloys, friction and wear mechanisms, initial behavior of tribo-corrosion, nitrogen ion implantation

1. Introduction

CoCrMo alloys have been widely and successfully used for orthopedic implants, such as hip and knee joints, because of their excellent biocompatibility, corrosion and wear resistance due to mixed passive oxide films of chromium and cobalt oxides that form spontaneously on the alloy surface (Ref 1-3). In human body, the implant surfaces come into direct contact with host tissues, resulting in passive dissolution, which limits long term use of the CoCrMo alloys. CoCrMo alloys tend to wear and corrode, releasing metal ions and metallic wear debris into body fluids over time, which results in implant failure, osteolysis and allergic reactions (Ref 4). A number of studies have been carried out to improve the alloy surface performance. Türkan et al. (Ref 4) reported that TiN coating deposited by physical vapor deposition (PVD) at 550 °C for 6 h is an effective barrier to cobalt and chromium metal ions release from the CoCrMo alloy. Espallargas (Ref 5) treated forged CoCrMo alloy by pulsed plasma in a N^2/H^2 atmosphere at low temperatures. Guo et al. (Ref 6) used nitrogen ion implantation technique to modify the surface properties of medical grade CoCrMo alloy, and both of the results show that surface plasma treatment could improve tribo-corrosion of CoCrMo alloy. Liu et al. (Ref 7) deposited diamond like carbon (DLC) film on CoCrMo alloy by using filtered cathodic vacuum arc technique (FCVA). These coatings effectively improved wear and corrosion properties, and reduced the release of Co, Cr and Mo metal ions, along with the wear debris. However, no studies focused on the initial wear (running-in) stage and protein adsorption of the modified CoCrMo alloy in the tribo-corrosion system.

The wear rate increases and small wear debris are created during the running-in crucial stage. Based on clinical examinations, the amount of metal ions increased dramatically in the first few days after CoCrMo joints implantation (Ref 8). In a previous study (Ref 6), it was found that the open circuit potential and the coefficient of friction exhibit similar sharp simultaneous changes, indicating that the modified layer has been worn through. Conditions where nitrogen ion-implanted layer was not worn through as the initial wear stage were also defined. However, the sample still had excellent wear resistance and corrosion resistance after the modified layer failure. Dienes et al. (Ref 9, 10) considered a new phase formation outside the surface injection layer due to hot blasting and internal stress in the local area. Hartley et al. (Ref 11, 12) argued that wear promotes nitrogen ions diffusion into deeper matrix layers before the nitrogen ion implantation layer was removed. There is a limited number of reports focusing on friction with bovine serum albumin (BSA) adsorption. The study (Ref 13) has shown that the BSA adsorption provides lubrication and can reduce friction. In this paper, the change of BSA adsorption induced by nitrogen ions implantation is considered as one of the reasons causing this phenomenon.

When biomaterials are placed in a living body, protein adsorption plays an important role in physiological consequences of biomaterial implantation, including coagulation, thrombogenesis, acute and chronic inflammatory responses (Ref 2). Proteins interact with metal ions released from biomaterials, generating complex organic–metallic biofilms. These biofilms can reduce friction by acting as lubricating films (Ref 13). Protein adsorption directly affects the service life of biological materials; thus, studying protein adsorption behavior

Xueyan Yan, Jie Meng, Kewei Gao, and **Xiaolu Pang**, School of Materials Science and Engineering, University of Science and Technology Beijing, Beijing 100083, China; **Alex A. Volinsky**, Department of Mechanical Engineering, University of South Florida, Tampa, FL 33620. Contact e-mail: pangxl@mater.ustb.edu.cn.

in these material systems is essential. Valero-Vidal et al. (Ref 14, 15) studied the effects of BSA on composition and thickness of the surface passive film on CoCrMo alloy, and investigated the effects of temperature and protein concentration on BSA adsorption behavior. There are no relevant reports of BSA adsorption on modified surfaces. Most BSA adsorption studies focus on static conditions, which are far away from the actual conditions. In this work (Part I), BSA adsorption conditions in the tribo-corrosion system were established using fluorescence labeling. In part II, the effects of nitrogen ion implantation on tribo-corrosion behavior of CoCrMo alloy were studied during the initial wear stage. The relationships between tribo-corrosion behavior and BSA adsorption on nitrogen ion-implanted CoCrMo alloy in the tribo-corrosion cell are also discussed.

2. Experimental Details

2.1 Sample Preparation and Nitrogen Ion Implantation

The metal used in this study was medical grade CoCrMo (Co-27.7Cr-5.7Mo-0.05C-0.17N-0.24Fe (in wt.%)) alloy (ASTM F-75). The ingot was cut into small samples with 20 mm diameter, 5 mm thick. All samples were prepared using the same process. The samples were grounded by different types of sandpaper, from 500# to 5000#, and then mechanically polished to make the surface to mirror-like. After that, ultrasonically cleaned for 20 min in acetone, ethanol, and deionized water and dried using warm air prior to testing.

Nitrogen ion implantation is a surface modification technique generally accepted to enhance wear and corrosion resistance and has been widely applied to improve biomedical materials properties (Ref 6, 16-20). Before implantation all specimens were sputter cleaned with argon ions at 5 keV to remove residual surface contaminants. Nitrogen ions were implanted into the polished specimens in the vacuum chamber with 2×10^{17} N^+/cm^2 dose at 100 keV. During implantation the vacuum chamber was not heated to keep low temperature to avoid changing the alloy microstructure. Nitrogen ions were generated using electron cyclotron resonance with 1000 W power and 2.45 GHz frequency.

2.2 Surface Characterization

3D optical profiler was used to observe the surface morphology of both polished (un-implanted) and N-implanted CoCrMo alloys. The grazing incidence technique (GIXRD) was used to obtain the implanted layer phases at the grazing angle of 1° with CuK_α radiation (λ = 1.5404 Å) at a scanning rate of 3°/min. Nanoindentation measurement was carried out to evaluate the hardness of samples with and without ion implantation using Nano Indenter. Continuous stiffness mode (CSM) was used to measure the hardness with the increase in indentation depth (Ref 21). The indenter has a Berkvoich indenter with tip curvature radius of 120 nm. The constant strain rate of 0.05/s was set for all samples. It offers a direct measure of the hardness change with the indentation depth. Mechanical properties of the substrate and nitrogen-implanted layers were characterized by nanoindentation.

2.3 BSA Adsorption

The surface morphology, composition and structure of the CoCrMo alloy were changed by N ion implantation, which in turn affects the BSA adsorption. Contact angle reflects interactions between the solid and liquid. The wetting of the samples tested in this paper was determined by the contact angle method with the BSA solution of 2 mg/ml (Ref 22). The contact angle of each sample was measured by the average of three positions with the drop volume of 2 µl.

BSA adsorption test in dynamic environment was carried out by using the fluorescent tags method with fluorescein isothiocyanate (FITC). FITC is orange yellow crystalline powder of $C_{21}H_{11}NO_5S$ with 389.4 molecular weight.

In alkaline conditions, the isothiocyano group of FITC molecules (–n=C=S) can react with free amino groups in protein molecules through the acylation reaction to form carbon sulfur amino keys, called fluorescent protein markers.

$$\begin{aligned} \mathrm{FITC-N=C=S+N-H_2-protein} \\ \rightarrow \mathrm{FITC-NH-S-C-N-H-protein} \end{aligned}$$

FITC was dissolved in carbonate buffer solution (pH = 9, 0.5 mol/L) forming 1 mg/ml FITC solution mixture in the dark. Take 40 mg BSA into colorimetric tube, then add 1.5 ml water, 0.5 ml carbonate buffer solution in turn and 1 ml FITC solution slowly. The solution was placed in the refrigerator for 12 h at 4 °C to react while avoiding light. BSA adsorption test in the dynamic environment was conducted in the reciprocating tribological tester. The samples were subjected to 5 N normal load applied with a 5 mm diameter Si_3N_4 ball for 5 min in the FITC-BSA solution at room temperature. The stroke length was 15 mm. After experiments, all samples were immersed in deionized water for 1 min to remove residual FITC-BSA, dried in the air and then observed under the fluorescent microscope.

2.4 Tribo-corrosion Tests

One of the factors that influence wear is lubrication. Due to comparable amounts of proteins and amino acids in the joint fluid, bovine calf serum was employed to simulate the synovial fluid and study tribo-corrosion properties of the CoCrMo alloy. In the tribo-corrosion system, the total material loss is induced by wear, corrosion and wear-corrosion interactions, since the combined effects of corrosion and wear can exceed their corresponding individual contributions (Ref 5, 23, 24).

Ball-on-plate wear tests are commonly used to characterize the surface performance under simulated conditions, although they cannot exactly represent the real environment of implanted materials. In this paper, tribo-corrosion tests were conducted in the system comprised of a three-electrode cell of the counter electrode (platinum wire), the reference electrode (silver/silver chloride electrode) and the working electrode (tested materials), and a reciprocating tribological tester (Fig. 1). The samples were tested at a normal load of 5 N against a 5 mm diameter Si_3N_4 ball (due to its electrochemical stability) for different time. The stroke length was 15 mm. All tests were conducted at room temperature. In this study, before and after wear testing, the sample was immersed in the simulated fluid for 30 min to reach a steady surface state. The whole experiment was conducted under the open circuit potential (OCP). To explore the initial wear behavior, the N-implanted sample and the untreated ample were tested in the tribo-corrosion system for different time (sliding distance).

After the tribo-corrosion test, the wear track morphology and volume of the tested CoCrMo alloy were quantified by the 3D optical profiler and a confocal laser scanning microscope (CLSM) was used to observe the surfaces of the Si_3N_4 balls. Inductively coupled plasma mass spectrometer (ICP-MS) was used for measuring the concentrations of metal ions (Co and Cr) from collected grinding fluids after centrifuged and diluted with 4 vol.% HNO_3.

3. Results and Discussion

3.1 Morphology and Microstructure

Images of tested surface are shown in Fig. 2 and the surface roughness *Ra* is 13.6 nm without implantation, and it is 12.4 nm with 2×10^{17} N^+/cm^2 ions implantation. The surface roughness due to ion implantation is not obvious and can be neglected compared with the general commercial artificial hip joint surface roughness of 0.01 mm.

Grazing incidence x-ray diffraction of the tested samples was conducted at the incident angle of 1°, and the results are shown in Fig. 3. For the untreated sample, the structure appears to be a mixture of fcc-γ and hcp-ε cobalt parent phases with solid solution chromium and molybdenum, and there is higher γ/ε ratio. The fcc-γ phase is about 90% and the hcp-ε phase is about 10%, which are all solid solution phase containing Cr and Mo (Ref 25, 26). An important observation is disappearing of the fcc-γ and hcp-ε phases and the formation of the CrN phase after treatment. CrN is a hard compound phase, which increases the hardness and wear resistance of the nitrided CoCrMo alloy (Ref 26).

3.2 Nanoindentation Hardness

Figure 4 shows the hardness change with the indentation depth using the CSM technique. For the 2×10^{17} N^+/cm^2 dose, the hardness shows higher values compared with the untreated one, which may be caused by the formation of harder phases (CrN) in the implanted sample. The maximum indentation hardness values for the 2×10^{17} N^+/cm^2 and untreated one is 15.7 ± 1.33 and 11.25 ± 3.49 GPa, with the indentation depth is 56.1 and 60.8 nm, respectively. It is obvious that the hardness is still higher at the depth larger than the modified layer thickness (beyond 180 nm). This may be due to the new phase formation outside the surface injection layer because of the localized hot blast and internal stress effects (Ref 9, 10).

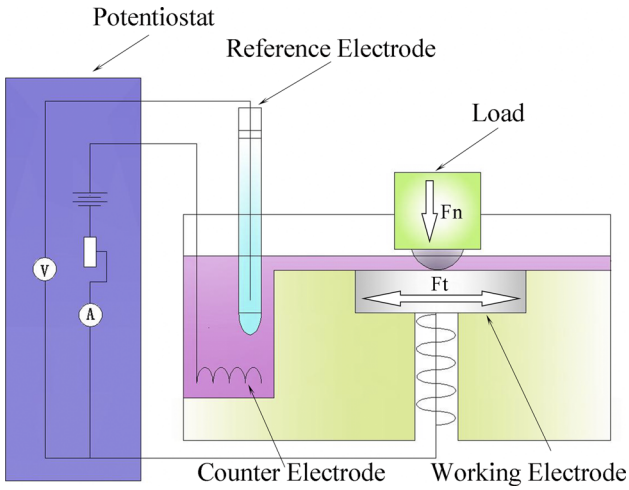

Fig. 1 Schematics of the tribo-corrosion system

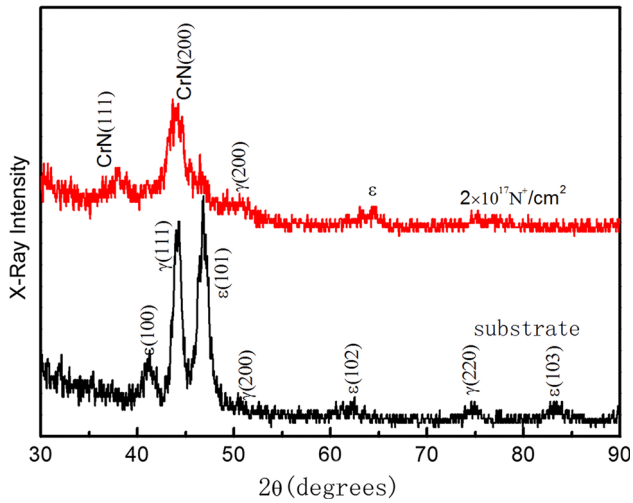

Fig. 3 GIXRD patterns of untreated and nitrided CoCrMo alloys

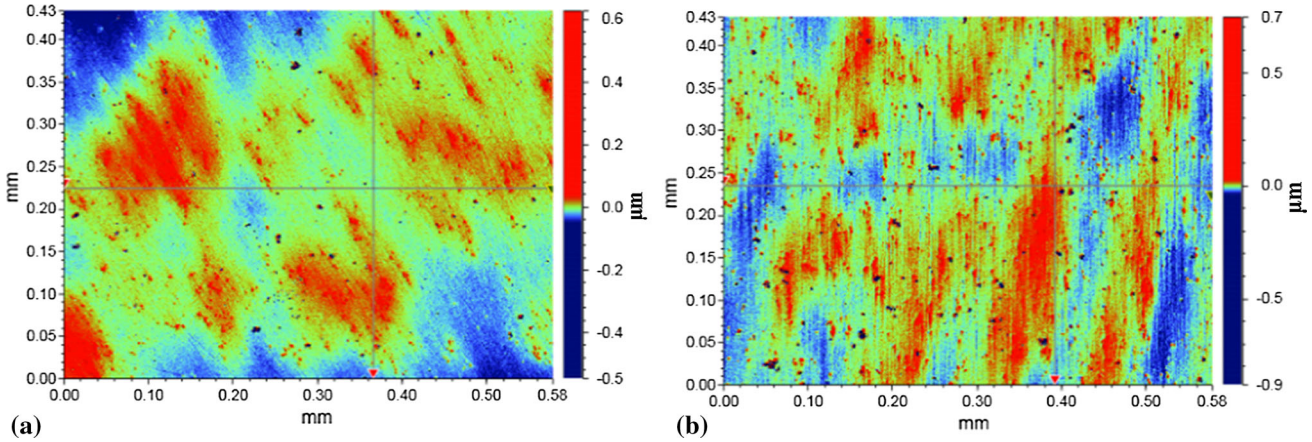

Fig. 2 Images of the sample surface: (a) un-implanted and (b) implanted with 2×10^{17} N^+/cm^2 dose

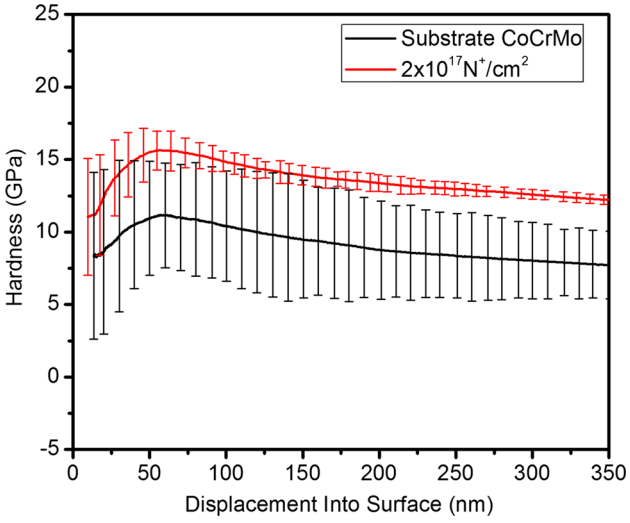

Fig. 4 Nanoindentation hardness of un-implanted and implanted samples

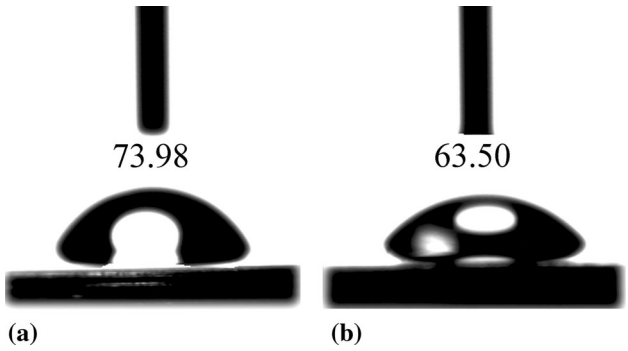

Fig. 5 Contact angle values of BSA solution on the tested sample surface: (a) substrate, (b) 2 × 10^{17} N^+/cm^2 N-implanted sample

3.3 BSA Adsorption

The contact angle values of BSA solution on the tested sample surface are shown in Fig. 5. It can be seen that after nitrogen ion implantation, the contact angle (63.50 ± 0.97°) is smaller than for the untreated sample (73.98 ± 1.01°), which suggests that the wettability of BSA solution on the modified layer is better. Thus, one can conclude that nitrogen ion implantation can improve the wettability of BSA solution on the CoCrMo alloy surface.

Figure 6 shows BSA dynamic adsorption results under the fluorescence microscope. The FITC-BSA adsorption of nitrogen ion implanted samples is obviously higher compared with the untreated one at the surface grinding track. Yan et al. (Ref 13) reported that the proteins can interact with metal ions to form organic–metallic biofilm. The biofilm can effectively reduce the wear volume and prolong the service life of materials. The grinding track width of nitrogen ion implanted samples is narrower than the untreated one. Thus, nitrogen ion implantation can improve CoCrMo alloy wear resistance. Compared with other areas, FITC-BSA adsorption is better at the grinding track, which shows that friction promotes BSA adsorption on the CoCrMo alloy surface and under certain pressure of friction is the main factors in the process of BSA dynamic adsorption. This result is similar to Myant's (Ref 28) research conclusion.

The contact angle values of BSA solution on the tested samples surface indicated that nitrogen ion implantation can improve the BSA solution wettability on the CoCrMo alloy surface. Meanwhile, the study of the BSA dynamic adsorption on the untreated and nitrided CoCrMo alloy surfaces was conducted, and the fluorescence microscopy results revealed that nitrogen ion implantation can promote BSA adsorption on the CoCrMo alloy surface in the simulated human body environment. This may be associated with the changes of the friction and wear mechanisms. In the running-in stage, the wear is serious and the proteins were peeled off with small wear debris into the fluid, so the proteins cannot have very good lubrication effect. The presence of protein in the metal-on-metal interface formed organic–metallic biofilm that can effectively reduce the wear volume and prolong the service life of materials as a lubricating film. Too much protein adsorption on the surface may be one of the reasons for the decreased wear rate after injection (Ref 6).

3.4 Tribo-corrosion Results

3.4.1 Wear Results. Figure 7 and 8(a)-(d) show the worn surface morphology and the wear track profiles of the untreated and nitrogen ion-implanted CoCrMo alloy. Morphology of the worn surfaces after different wear times is shown in Fig. 7 (figures above are the substrate sample, figures below are the implanted alloy). It is clear that the worn surfaces of the untreated CoCrMo alloy show sharp grooves compared with the worn surfaces of nitrogen ion-implanted ones, which exhibit shallower, relatively smooth grooves and fewer abrasion pits. The wear track width and depth of nitrogen ion-implanted samples is narrower than the untreated ones until after 4 h of wear. The wear track volumes of untreated and nitrogen ion-implanted CoCrMo alloy are shown in Fig. 8(e). With increasing the wear time, the nitrogen ion-implanted layers are worn through, but the samples treated by N ions implantation show excellent wear resistance performance, which can be seen from the images of the wear track profiles and the wear track volumes. The wear damage of silicon nitride balls as the counterpart after wear is shown in Fig. 9 (right figures are the balls against the CoCrMo alloy substrate, left figures are the balls against the N 2 × 10^{17} N^+/cm^2 sample). The surface of the balls sliding with the nitrogen ion-implanted CoCrMo alloy exhibits shallower, relatively smooth grooves and fewer abrasion pits.

From the images of the sliding surface (plate and ball), the friction and wear mechanisms were changed in the tribo-corrosive system by the nitrogen ions implantation. The complete tribological process is quite complex because it involves simultaneous mechanical friction and wear mechanisms both at micro- and macroscales as well as chemical effects and material transfer (Ref 27). For the 2 × 10^{17} N^+/cm^2 dose, the sliding surface is relatively smooth during 1 h wear, indicating adhesive wear domination. With increasing wear time, a lot of scratches were observed, possibly caused by dominated abrasive wear. For the CoCrMo alloy, the wear was more serious compared with the nitrogen ion-implanted one. Only after 20 min wear time, the sliding surface exhibits shallower and relatively smooth grooves; then, the worn surface

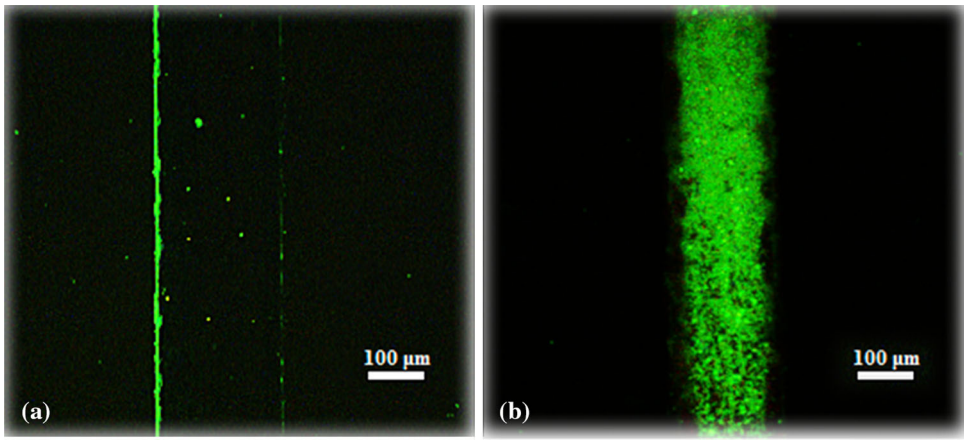

Fig. 6 BSA dynamic adsorption on the tested samples surface: (a) substrate, (b) 2×10^{17} N^{+}/cm^{2} sample

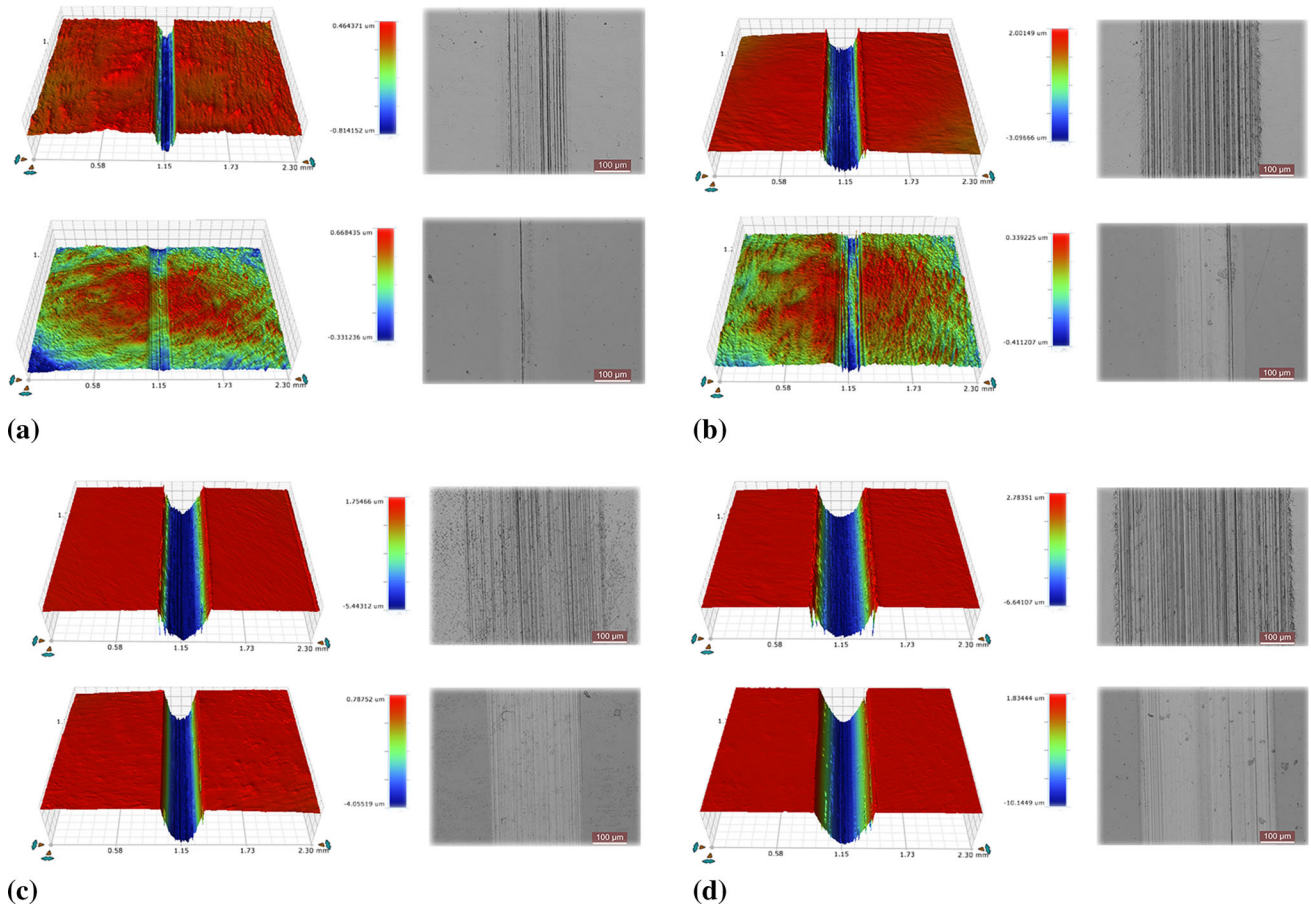

Fig. 7 Morphology of the worn surfaces with the substrate on top, and the 2×10^{17} N^{+}/cm^{2} N-implanted sample under it, after different wear times: (a) 20 min, (b) 1 h, (c) 2 h and (d) 4 h

shows lots of scratches with increased wear time. This indicates that the wear process of the substrate is faster into the severe wear stage than the nitrogen ion-implanted CoCrMo alloy and a large number of grinding debris peeled off from the material surface into the fluid, which may be one of the reasons effecting BSA adsorption.

From the observation for the friction pair morphology after tribo-corrosion tests, it is found that the friction and wear mechanisms were changed by N ions implantation. The wear process of the substrate is faster into the severe wear stage than the nitrogen ion implantation CoCrMo alloy and a large amount of debris came from the material surface into the fluid. In the

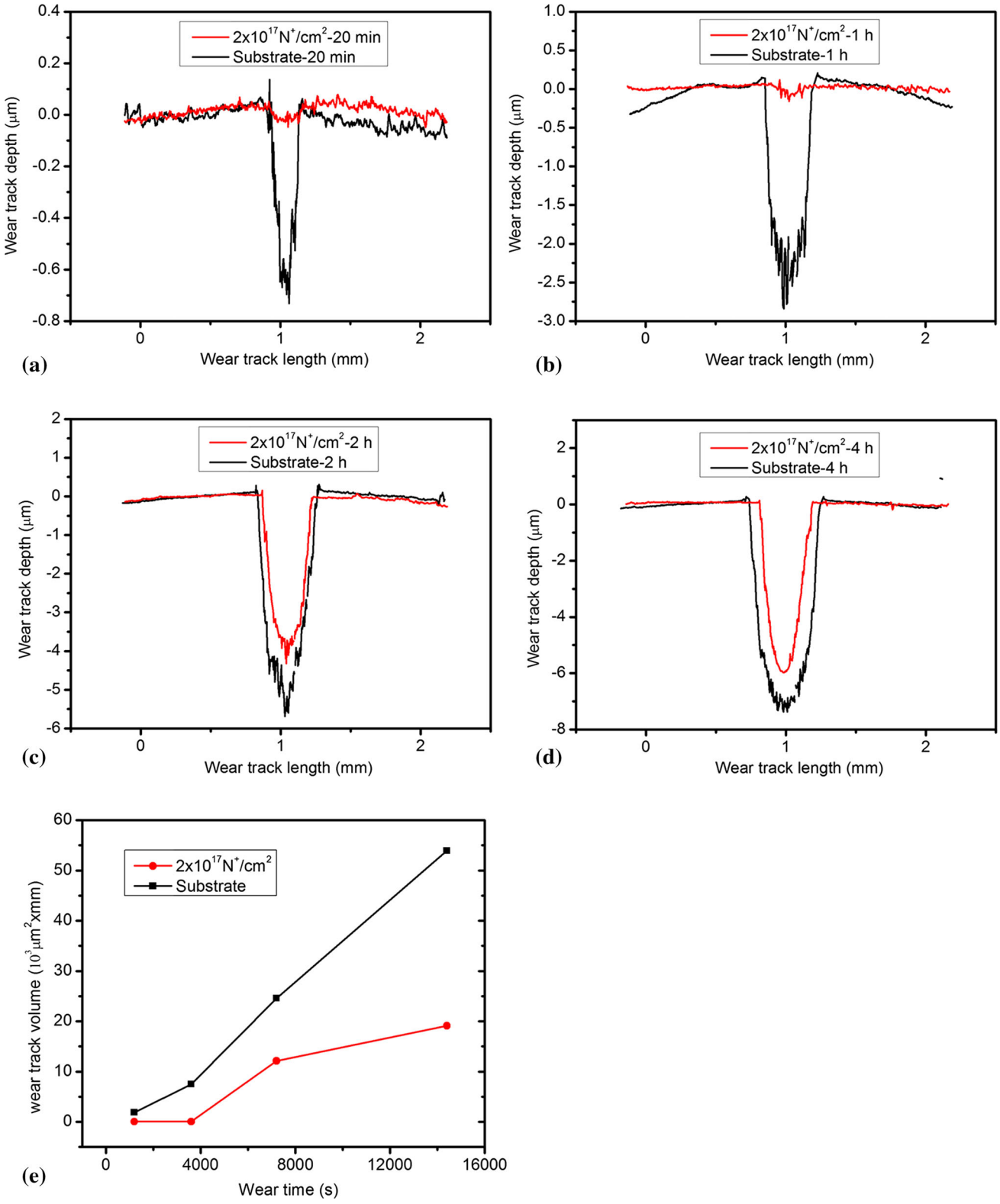

Fig. 8 Wear track profiles of substrate and with 2×10^{17} N^+/cm^2 N-implanted sample after different wearing time (a) 20 min; (b) 1 h; (c) 2 h; (d) 4 h; (e) wear volume of the CoCrMo alloy substrate and the N 2×10^{17} N^+/cm^2 sample after different wearing time

initial running-in stage, for the 2×10^{17} N +/cm^2 dose, the adhesive wear dominated, however, for the CoCrMo alloy base, the abrasive wear dominated resulting in higher wear volume.

3.4.2 Friction Coefficient and OCP. Figure 10 shows the evolution of the open circuit potential (OCP) and coefficient of friction (COF) for all samples with time in corrosive fluid

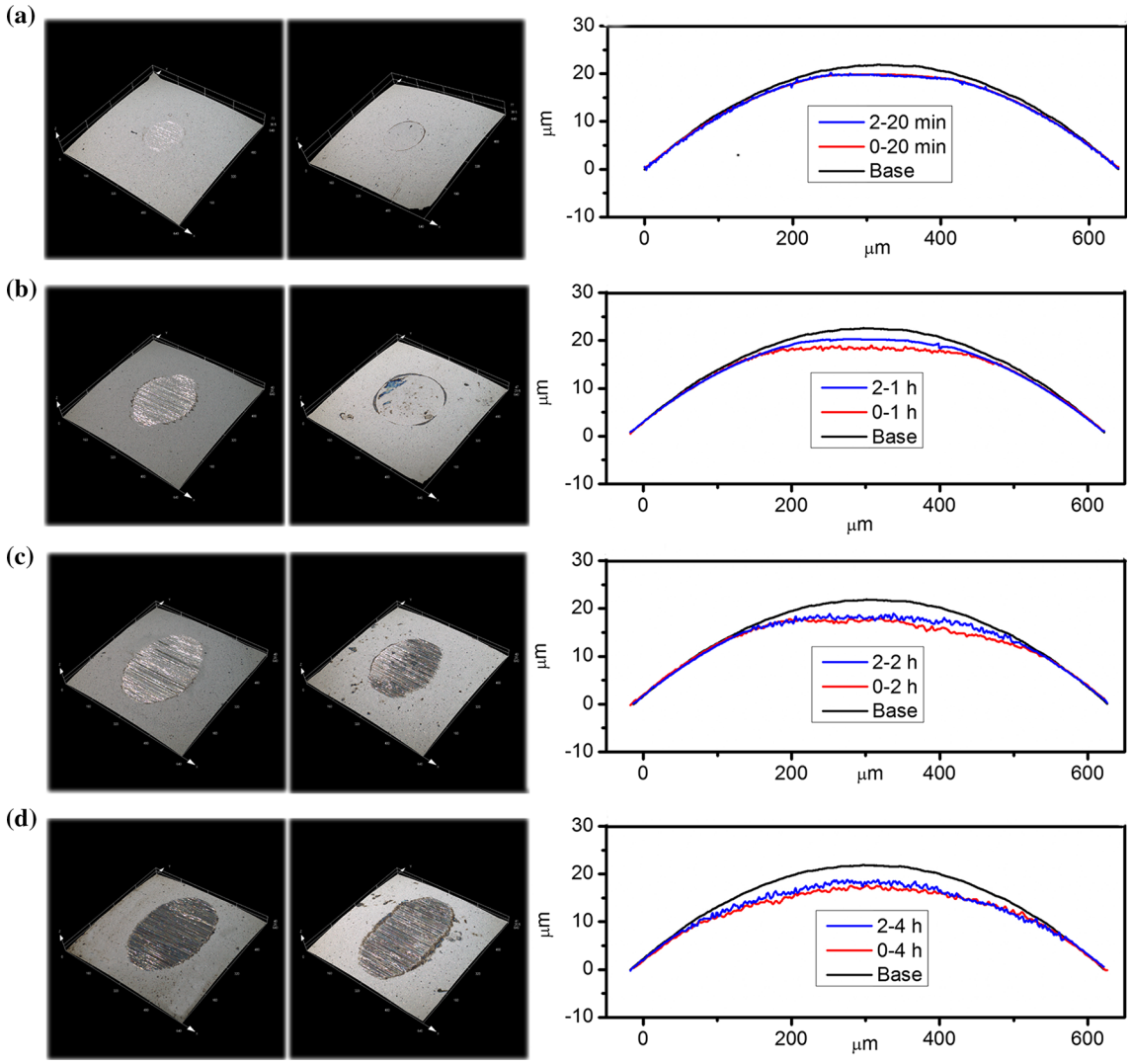

Fig. 9 Morphology for the wear damage of silicon nitride balls as the counterpart after different wear time. (a) 20 min, (b) 1 h, (c) 2 h and (d) 4 h

under sliding. The samples were submerged statically in the solution for 30 min before and after wear testing. The samples were worn at different times of 20 min, 1 h, 2 h and 4 h. The OCP measurements were conducted during the whole wear process. It can be seen in Fig. 10 that at the onset of wear, the OCP shifted to a more cathodic value (drop of 0.05 V) due to the removal of passive film (Ref 5, 23). The open circuit potential of the nitrided sample is more positive (above 0.6 V) compared with the untreated one after the onset of friction. Moreover, the COF for nitrogen ion implantation sample was lower compared with the untreated one, reaching 0.2. A similar behavior can be seen from the values of COF and OCP, exhibiting a transition before nitrogen ion implantation layer was worn through. With increasing wear time from 1 to 2 h and 4 h, a clear shift (Fig. 10(b-d)) can be seen after half an hour of sliding, indicating that the nitrogen ion implantation layer was removed, resulting in a decrease of OCP and an increase in COF until the nitrogen ion implantation layer was worn through. The potential and coefficient of friction reached a relatively stable region after the transition period when equilibrium was attained between the mechanical de-passivation rate and electrochemical re-passivation rate (Ref 7). The OCP of the nitrided sample is more positive (above 0.3 V) than the OCP of the untreated one, and the COF remained at around 0.3, which is lower compared with the COF of untreated sample after the modified layer failure. This indicates that the nitrogen ion-implanted CoCrMo alloy still shows excellent wear and corrosion resistance after the transition period. It is possible that wear promotes nitrogen ions migration into deeper matrix before the nitrogen ion implantation layer was removed (Ref 11, 12). Nitrogen ions implantation can further improve wear and corrosion resistance of base material during use. Combined with the BSA adsorption results, it can be concluded that nitrogen ions implantation can promote BSA dynamic adsorption due to the change of friction and wear mechanisms. D. Sun et al. (Ref 29) found the concentration of protein is a key impact to influence the erosion rate. High protein concentration profits to enhance the lubricating property. So,

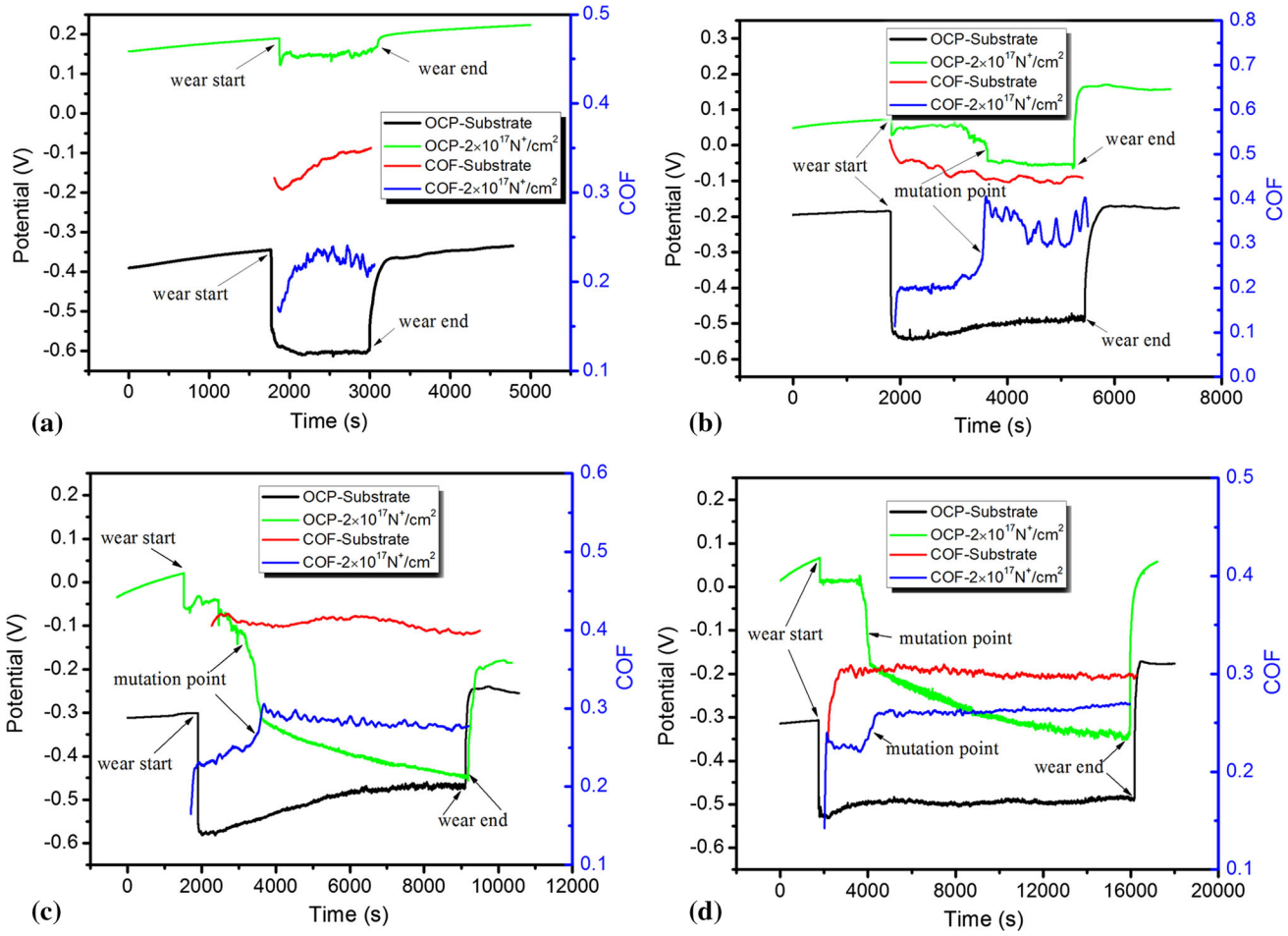

Fig. 10 Potential and friction coefficient evolution with time during tribo-corrosion tests in bovine serum at the open circuit potential of un-implanted and nitrogen ion-implanted 2 × 10^{17} N^+/cm^2 dose sample after different wear time: (a) 20 min, (b) 1 h, (c) 2 h, and (d) 4 h

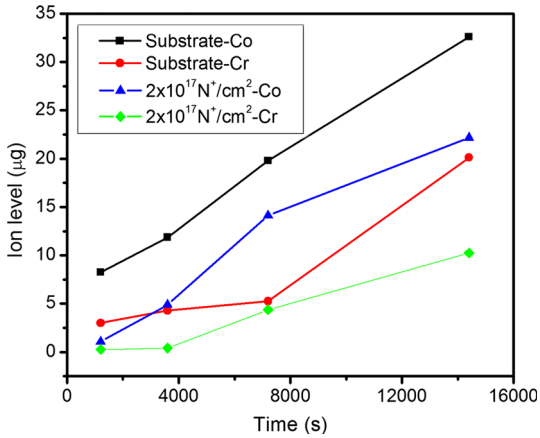

Fig. 11 Co and Cr ions concentrations released into the simulated body fluid during the tribo-corrosion test measured by ICP-MS

an increase in BSA adsorption can reduce the friction volume and block metal ions release. This means nitrogen ions implantation changed friction and wear mechanisms, which is one of the reasons of better BSA adsorption in the simulated environment. The BSA adsorption effectively reduced wear and corrosion.

3.4.3 Ion Concentration. The concentration of Co and Cr ions released into the simulated body fluid from the specimens was determined using ICP-MS and are shown in Fig. 11. The Co ion release behavior is quite similar with the Cr ion, and with the wear time, the concentration of released Co and Cr ions increase. For all samples, due to selective cobalt dissolution, the concentration of released cobalt ions is greater than the concentration of chromium ions. Despite of nitrogen ion implantation layer wear, the released amounts of Co and Cr ions released in solution from nitrogen ion implantation CoCrMo alloy are lower than for the CoCrMo alloy substrate. This is consistent with the above discussion.

It can be seen from the results of the tribo-corrosion test that at the onset of wear, the OCP dropped by 0.05 V due to the removal of passive film. Before failure of the modified layer, the open circuit potential of the nitrided sample is more positive (above 0.6 V) and the COF is lower (0.2), compared the untreated one. The OCP and COF all have a sharp change at the wear time about 30 min, named the transition point. After the modified layer failure, the OCP and COF became stable. The OCP of the nitrided sample rose by 0.3 V compared with the untreated sample, and the COF remained at around 0.3, which is lower compared with the untreated sample. The electro-chemical and tribology signals revealed that the nitrogen ion

implantation improved the wear resistance and corrosion resistance in the simulated body fluid. The quantity of ions released and wear track volumes also provide a strong evidence for the effect of the ion implantation on enhancing the corrosion and tribo-corrosion performance of the CoCrMo alloy. Meanwhile, the effect of nitrogen ions implantation on the wear and corrosion resistance of the base material further improved. The tribo-corrosion test results indicate that the nitrogen ion-implanted CoCrMo alloy still shows excellent wear and corrosion resistance after the layer was worn through. Combining the results of BSA adsorption, an increase in BSA adsorption induced by the change of friction and wear mechanisms due to nitrogen ions implantation conducted on the CoCrMo alloy surface, the BSA adsorption is one of the reasons that CoCrMo alloy still has excellent wear and corrosion resistance in the simulated environment.

4. Conclusions

As nitrogen ions were implanted into the CoCrMo alloys, the CrN phase formed, which improved wear and corrosion performance. The effect of nitrogen ions implantation on the CoCrMo alloy properties is further, the hardness and the tribo-corrosion results providing strong evidence. Nitrogen ion implantation can promote BSA dynamic adsorption due to the change of friction and wear mechanisms. This means the friction and wear mechanisms is one of the reasons of BSA adsorption in the simulated environment. Meanwhile, as the corrosive medium, the BSA interaction with metal ions forms complex organic–metallic biofilms, which can effectively reduce friction as a lubricating film and block the metal ions release. This may be one of the reasons why CoCrMo alloy still has excellent wear and corrosion resistance after the modified layer was worn through in the simulated environment.

Acknowledgements

This work was supported by National Nature Science Foundation of China (51771025) and the Beijing Nova Program (Z171100001117075).

References

1. K. Yamanaka, M. Mori, and A. Chiba, Effects of Nitrogen Addition on Microstructure and Mechanical Behavior of Biomedical Co-Cr-Mo Alloys, *J. Mech. Behav. Biomed. Mater.*, 2014, **29**, p 417–426
2. C. Valero Vidal and A. Igual Muñoz, Study of the Adsorption Process of Bovine Serum Albumin on Passivated Surfaces of CoCrMo Biomedical Alloy, *Electrochim. Acta*, 2010, **55**, p 8445–8452
3. L.J. Zhao, W. Zai, M.H. Wong, and H.C. Man, Hydrothermal Synthesis of Ag-ZrO_2/r-GO Coating on CoCrMo Substrate, *Mater. Lett.*, 2018, **228**, p 314–317
4. Uğur Türkan, Orhan Öztürk, and Ahmet E. Eroğlu, Metal Ion Release from TiN Coated CoCrMo Orthopedic Implant Material, *Surf. Coat. Technol.*, 2006, **200**, p 5020–5027
5. A. Bazzoni, S. Mischler, and N. Espallargas, Tribocorrosion of Pulsed Plasma-Nitrided CoCrMo Implant Alloy, *Tribol. Lett.*, 2013, **49**, p 157–167
6. Z. Guo, X. Pang, Y. Yan, K. Gao, A.A. Volinsky, and T.-Y. Zhang, CoCrMo Alloy for Orthopedic Implant Application Enhanced Corrosion and Tribocorrosion Properties by Nitrogen Ion Implantation, *Appl. Surf. Sci.*, 2015, **347**, p 23–34
7. J. Liu, X. Wang, B.J. Wu, T.F. Zhang, Y.X. Leng, and N. Huang, Tribocorrosion Behavior of DLC-Coated CoCrMo Alloy in Simulated Biological Environment, *Vacuum*, 2013, **92**, p 39–43
8. Y. Yan, A. Neville, and D. Dowson, Biotribocorrosion—An Appraisal of the Time Dependence of Wear and Corrosion Interactions: I, The Role of Corrosion, *J. Phys. D Appl. Phys.*, 2006, **39**, p 3200–3205
9. G.J. Dienes, G.H. Vineyard, Radiation efects in solids, Interscience Publ., 1957
10. E. Johnson, T. Wohlenberg, and W. Grant, Crystalline Phase Transitions Produced by Ion Implantation, *Phase Transit. A Multinatl. J.*, 1979, **1**, p 23–33
11. N. Hartley, Friction and Wear of Ion-Implanted Metals—A Review, *Thin Solid Films*, 1979, **64**, p 177–190
12. P. Goode, A. Peacock, and J. Asher, A Study of the Wear Behaviour of Ion Implanted Pure Iron, *Nucl. Instrum. Methods Phys. Res.*, 1983, **209**, p 925–931
13. Y. Yan, A. Neville, and D. Dowson, Biotribocorrosion of CoCrMo Orthopaedic Implant Materials—Assessing the Formation and Effect of the Biofilm, *Tribol. Int.*, 2007, **40**, p 1492–1499
14. C. Valero-Vidal, A. Igual-Munoz, C.O.A. Olsson, and S. Mischler, Adsorption of BSA on Passivated CoCrMo PVD Alloy: An EQCM and XPS Investigation, *J. Electrochem. Soc.*, 2014, **161**, p C294–C301
15. C. Valero Vidal, A. Olmo Juan, and A. Igual Munoz, Adsorption of Bovine Serum Albumin on CoCrMo Surface: Effect of Temperature and Protein Concentration, Colloids and Surfaces. B, *Biointerfaces*, 2010, **80**, p 1–11
16. P. Budzynski, A.A. Youssef, and J. Sielanko, Surface Modification of Ti-6Al-4V Alloy by Nitrogen Ion Implantation, *Wear*, 2006, **261**, p 1271–1276
17. M.S. Oskooie, M.S. Motlagh, and H. Aghajani, Surface Properties and Mechanism of Corrosion Resistance Enhancement in a High Temperature Nitrogen Ion Implanted Medical Grade Ti, *Surf. Coat. Technol.*, 2016, **291**, p 356–364
18. X.B. Tian, C.B. Wei, S.Q. Yang, R.K.Y. Fu, and P.K. Chu, Corrosion Resistance Improvement of Magnesium Alloy Using Nitrogen Plasma Ion Implantation, *Surf. Coat. Technol.*, 2005, **198**, p 454–458
19. S. Ge, Q. Wang, D. Zhang, H. Zhu, D. Xiong, C. Huang, and X. Huang, Friction and Wear Behavior of Nitrogen Ion Implanted UHMWPE Against ZrO_2 Ceramic, *Wear*, 2003, **255**, p 1069–1075
20. R.A.S.E. Leitâo and M.A. Barbosa, Electrochemical and Surface Modifications on N+ -ion-Implanted 316 L Stainless Steel, *J. Mater. Sci. Mater. Med.*, 1997, **8**, p 365–368
21. B.B. Xiaodong Li, A Review of Nanoindentation Continuous Stiffness Measurement Technique and Its Applications, *Mater. Charact.*, 2002, **48**, p 11–36
22. L. Qin, P. Lin, Y. Zhang, G. Dong, and Q. Zeng, Influence of Surface Wettability on the Tribological Properties of Laser Textured Co-Cr-Mo Alloy in Aqueous Bovine Serum Albumin Solution, *Appl. Surf. Sci.*, 2013, **268**, p 79–86
23. D. Royhman, J.C. Yuan, T. Shokuhfar, C. Takoudis, C. Sukotjo, and M.T. Mathew, Tribocorrosive Behaviour of Commonly Used Temporomandibular Implants in a Synovial Fluid-Like Environment: Ti-6Al-4V and CoCrMo, *J. Phys. D Appl. Phys.*, 2013, **46**, p 1–9
24. M.T. Mathew, M.J. Runa, M. Laurent, J.J. Jacobs, L.A. Rocha, and M.A. Wimmer, Tribocorrosion Behavior of CoCrMo Alloy for Hip Prosthesis as a Function of Loads: A Comparison Between Two Testing Systems, *Wear*, 2011, **271**, p 1210–1219
25. Y. Okazaki, Effects of Heat Treatment and Hot Forging on Microstructure and Mechanical Properties of Co-Cr-Mo Alloy for Surgical Implants, *Mater. Trans.*, 2008, **49**, p 817–823
26. Q. Wang, L. Zhang, and J. Dong, Effects of Plasma Nitriding on Microstructure and Tribological Properties of CoCrMo Alloy Implant Materials, *J. Bionic Eng.*, 2010, **7**, p 337–344
27. K. Holmberg, A Concept for Friction Mechanisms of Coated Surfaces, *Surf. Coat. Technol.*, 1992, **56**, p 1–10
28. C. Myant, R. Underwood, J. Fan, and P.M. Cann, Lubrication of Metal-on-Metal Hip Joints: The Effect of Protein Content and Load on Film Formation and Wear, *J. Mech. Behav. Biomed. Mater.*, 2012, **6**, p 30–40
29. D. Sun, J.A. Wharton, and R.J.K. Wood, Effects of Proteins and pH on Tribocorrosion Performance of Cast CoCrMo—A Combined Electrochemical and Tribological Study, *Tribol. Mater. Surf. Interfaces*, 2008, **2**, p 150–160